Electronic Supplementary Material (ESI) for Journal of Materials Chemistry A.


# $MnP_4$ electrode for Na-ion batteries: a complex and effective electrochemical mechanism

Julien Fullenwarth,[a] Bernard Fraisse,[a] Nicolas Dupré,[b] Lorenzo Stievano, [a,c] Laure Monconduit[a,c, *]

[a] *ICGM, Univ. Montpellier, CNRS, ENSCM, 34293 Montpellier Cedex 5, France*

[b]*Institut des Matériaux Jean Rouxel (IMN), CNRS UMR 6502, Univ. Nantes, 44322 Cedex 3 Nantes, France*

[c]*Réseau sur le Stockage Electrochimique de l'Energie (RS2E), FR CNRS 3459, France*

## *Supplementary Information*

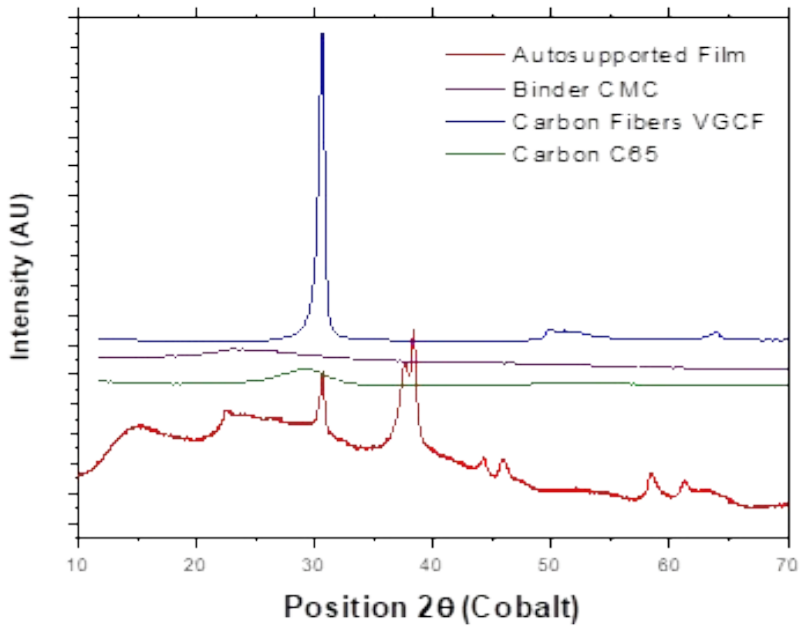


**Figure SI 1**: X-ray characterization (Co) of $MnP_4$ powder sample.

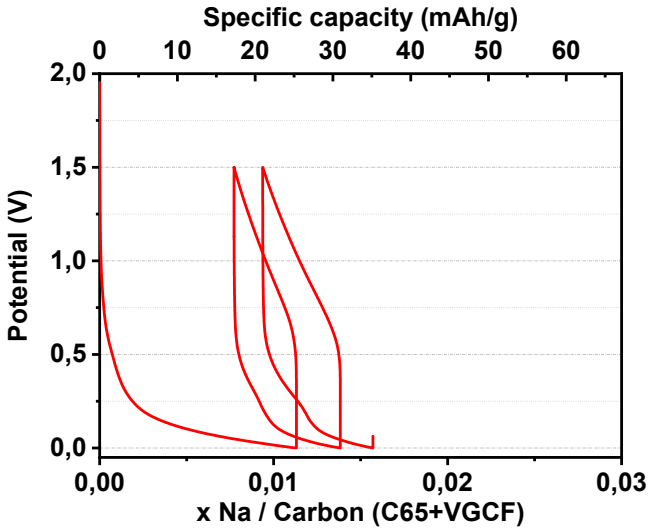


**Figure SI 2**: 1st galvanostatic cycles of carbon additives (C65/VGCF)(1:1)/Na

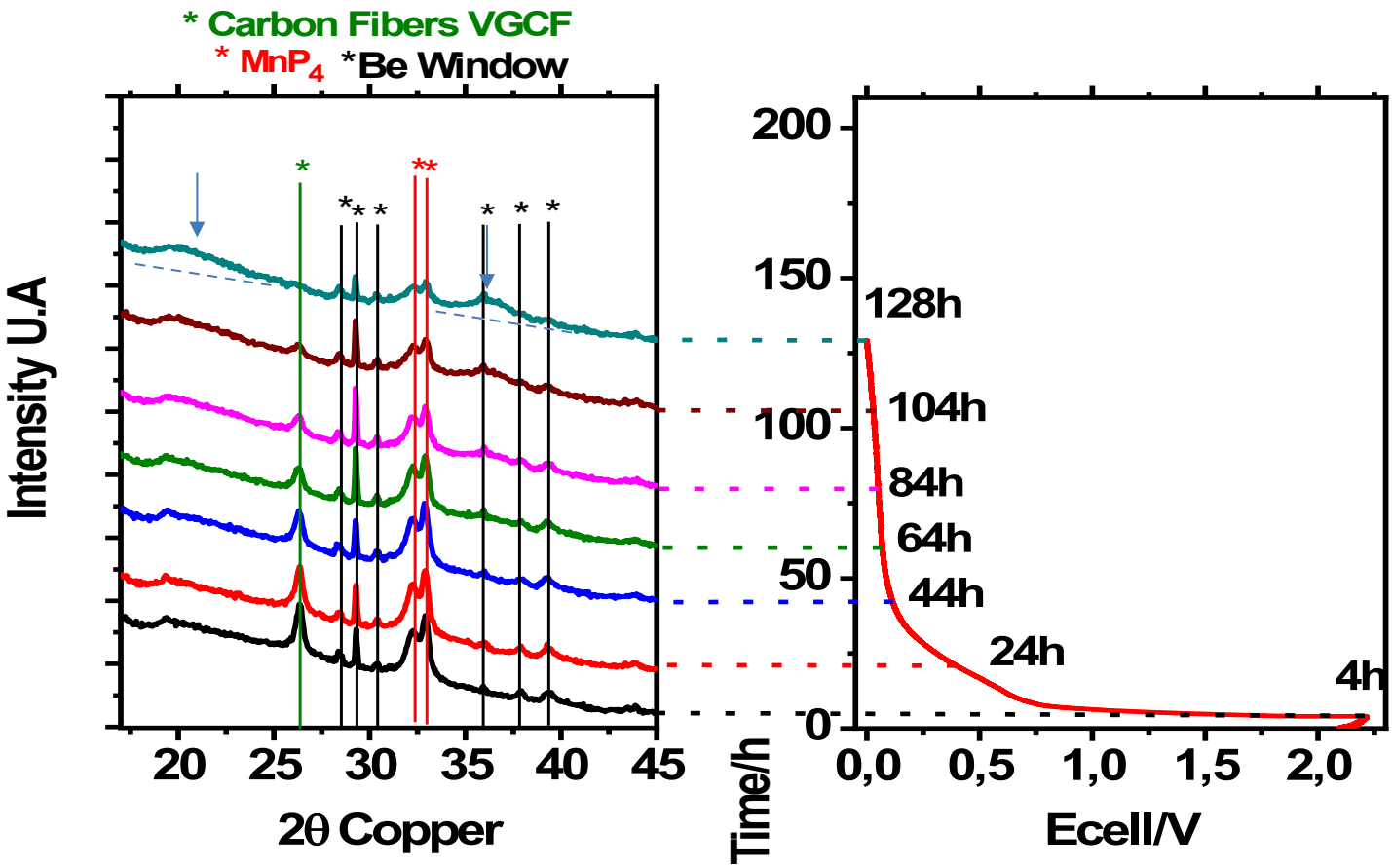


**Figure SI 3:** (a) XRD operando of $MnP_4$/Na cell during the first discharge at C/20 and associated galvanostatic curve.

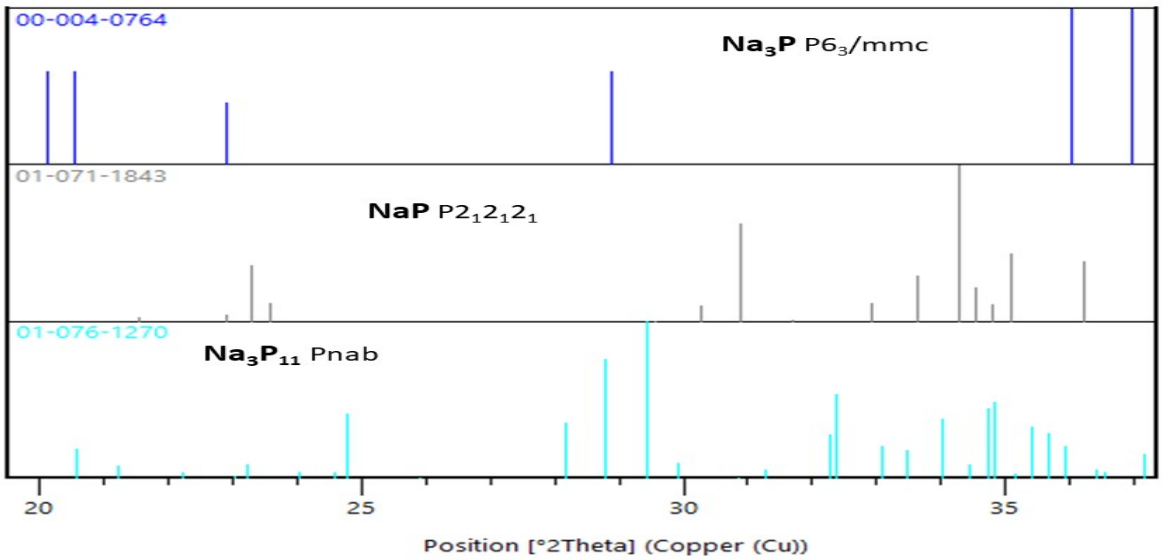


**Figure SI 4**: XRD patterns of different $Na_xP$ polymorphs reported in the ICSD database.

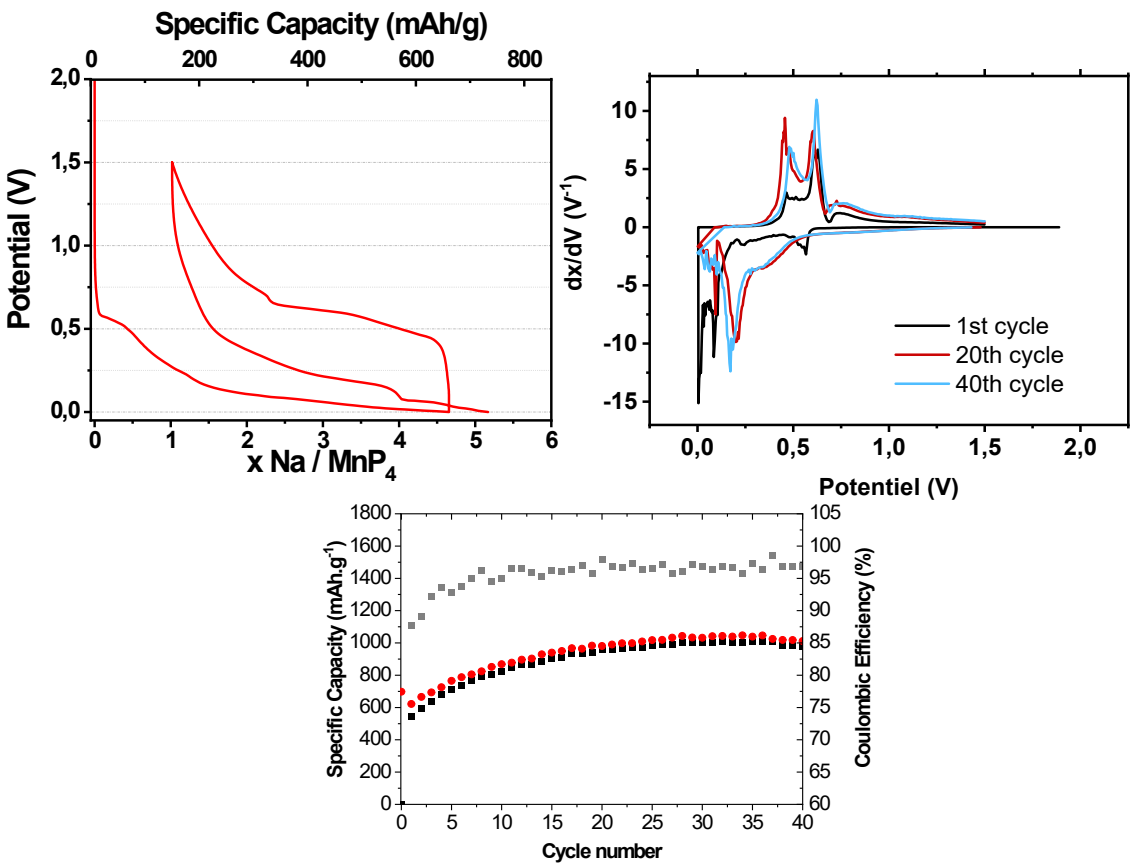


**Figure SI 5:** (a) First galvanostatic cycle and (b) corresponding derivative curve (1st cycle in black, 20th and 40th cycle in red and blue respectively) of a $MnP_4$/Na cell, with 74% of AM.

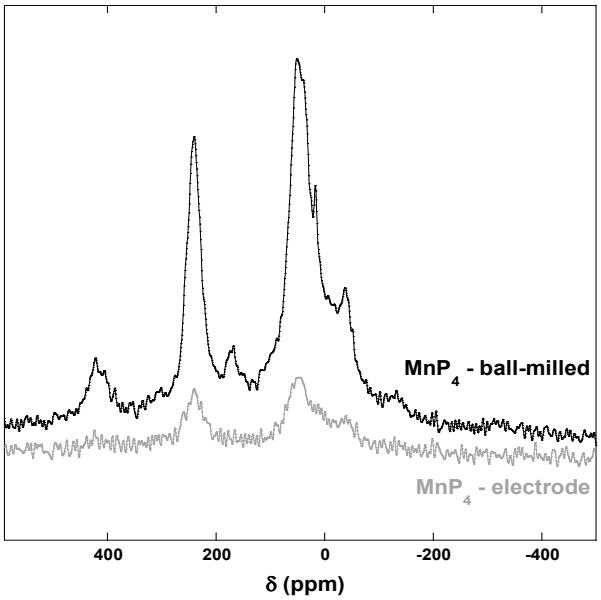


**Figure SI 6**: Normalized $^{31}P$ MAS NMR spectra for the pristine $MnP_4$ directly obtained from the ball-mill synthesis and the $MnP_4$ electrode (63 wt% of active material).

Figure SI 6 display the $^{31}P$ MAS NMR spectra for the pristine $MnP_4$, as obtained by ball-milling synthesis and the pristine $MnP_4$ after the electrode preparation. The Two spectra were obtained with a comparable number of scans and illustrate the loss of signal due to the effect of R.F. pulse dissipation due to the presence of conductive carbon.

**Observation of surface phosphates phases using MAS NMR**

In addition to the resonances linked with the electrochemical reaction of sodium and $MnP_4$, two resonances appear at 5 and 10 ppm and are assigned to surface phosphates that have possibly reacted with the electrolyte. The small but sharp resonance detected on the $^{31}P$ MAS NMR spectrum of the pristine $MnP_4$ at 16 ppm (Fig. SI 6), could correspond to native surface phosphates before any reaction with the electrolyte. The resonance at 16 ppm is replaced by a signal at -1 ppm on the $^{31}P$ NMR spectra of electrodes prior to cycling indicating that the electrode processing step has led to $MnP_4$ surface modifications. Nevertheless, a simple contact with the electrolyte does not seem to bring further change (Fig. SI 7). The additional shift observed for this resonance, to 5-10 ppm seems then to be the result of a redox reaction involving surface species upon the first lithiation process. Finally, resonances at 5-10 ppm are still present on the spectrum of

the electrode recovered at the end of the first cycle (1.5V) (Fig. SI 7), indicating that this surface species reaction is irreversible. Note that other resonances in this chemical shift range, usually assigned to phosphates may be present in the $^{31}P$ MAS NMR spectrum of the pristine $MnP_4$ but masked by the broad and intense signal of the bulk material.

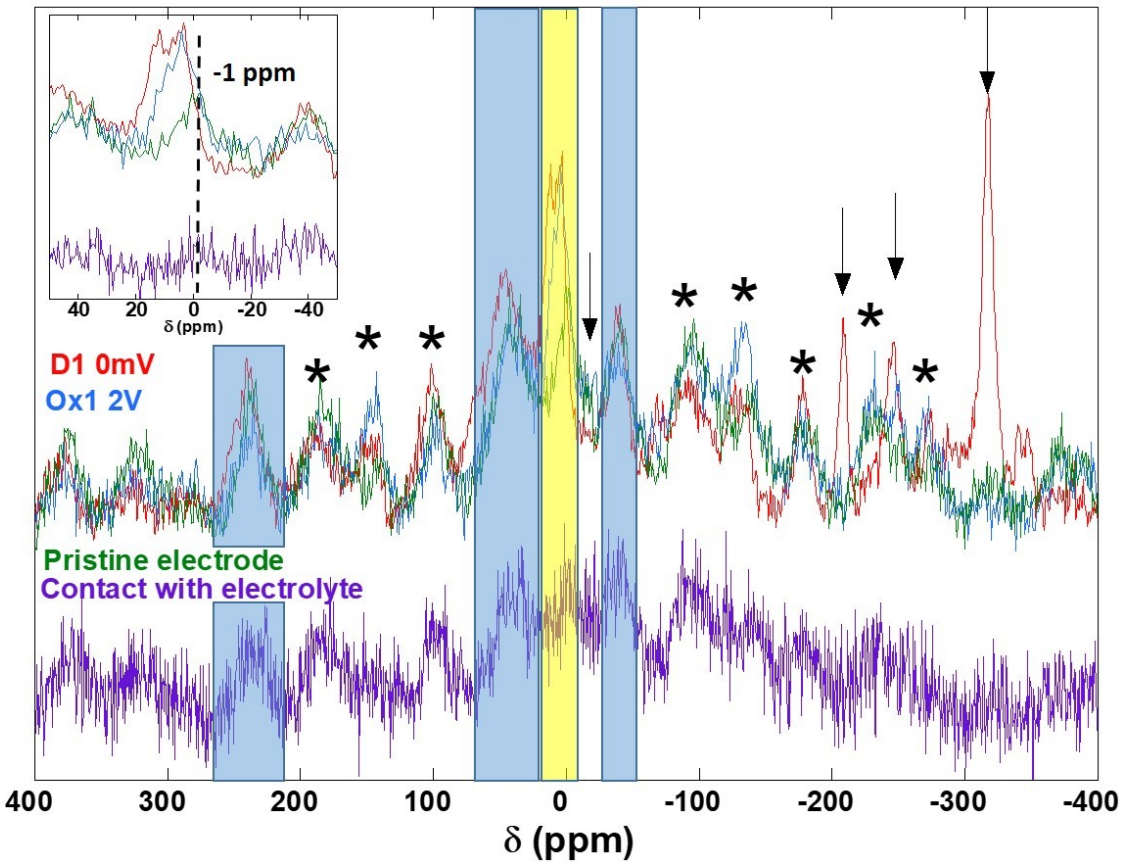


**Figure SI 7**: $^{31}P$ MAS NMR spectra for $MnP_4$ electrodes in its pristine state (green), after contact with the electrolyte (purple) after the first discharge to 0V (red) and the subsequent charge to 1.5V (blue) (74 wt% of active material). Asterisks correspond to spinning sidebands. The black arrows mark the position of identified sodiated phases. The blue areas mark resonances for the initial $MnP_4$. The yellow area marks resonances assigned to surface phosphates. They are shown enlarged in the inset.

## Identification of intermediate sodiated phosphides

We propose here a detailed attempt at identifying the intermediate sodiated phases and their stoichiometry. For both 63 wt.% and 74 wt.% electrodes, expected intense $Na_3P_{11}$ resonances at 150 and 170 ppm are not observed in our experimental spectra (Figure 7). While some of the $Na_3P_{11}$ characteristic resonances usually observed between -200 and -240 ppm could be masked by other broad signals in this region, there is no clear evidence of crystallized $Na_3P_{11}$ in discharged samples. Similarly, $Na_3P_7$ ($Na_{0.429}P$) resonances calculated between -57 and -188 ppm[29] or observed between -44 and -160 ppm[28] were not observed on our experimental spectra. Overall, Na and P environments similar to those in crystallized $Na_3P_7$ or $Na_3P_{11}$ cannot be ruled out in the discharged electrodes, but no clear evidence of the corresponding crystallized phases could be determined and our experimental results are more consistent with the presence of amorphous and disordered environments.

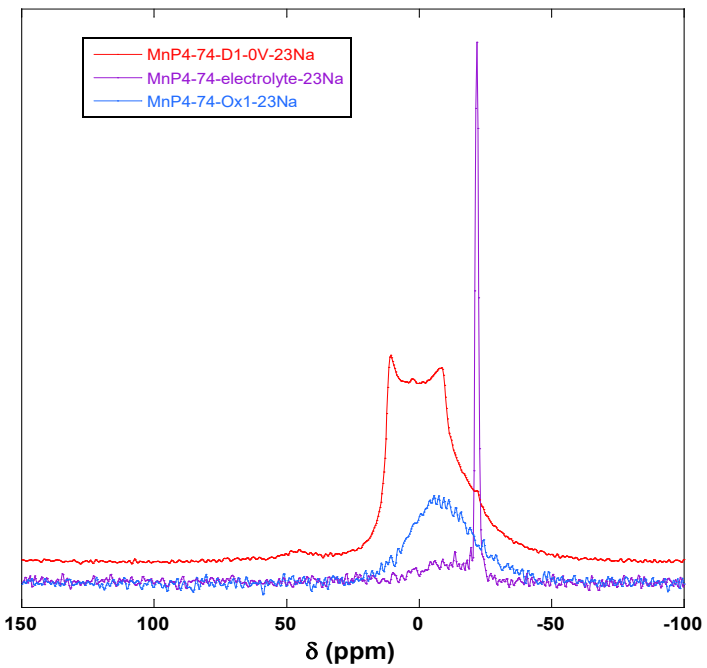


**Figure SI 8**: $^{23}Na$ MAS NMR spectra for $MnP_4$ electrodes after contact with the electrolyte (purple) after the first discharge to 0V (red) and the subsequent charge to 1.5V (blue) (74 wt% of active material).

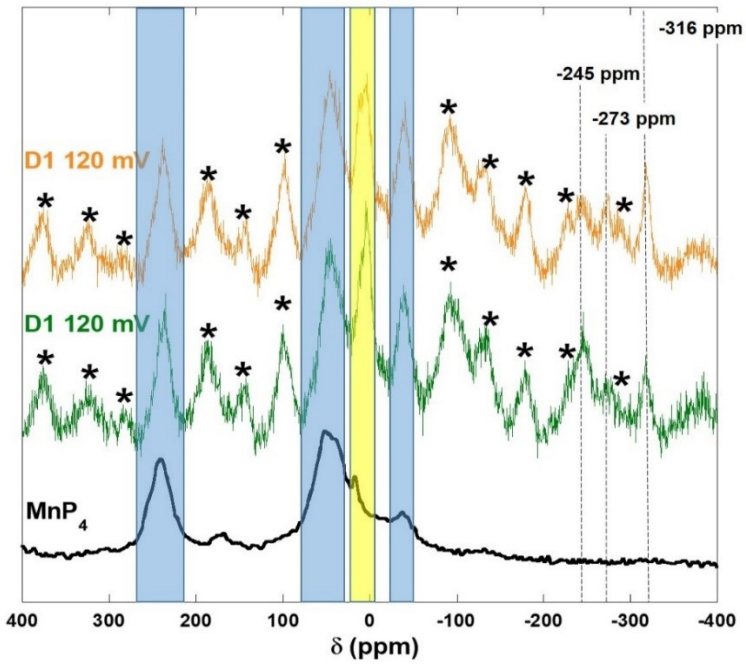


**Figure SI 9**: Normalized $^{31}P$ MAS NMR spectra of $MnP_4$ electrodes containing 63 wt% (orange) and 74 wt% (green) of active material, stopped at 120 mV during the first discharge. Asterisks correspond to spinning sidebands. The blue areas mark resonances for the initial $MnP_4$. The yellow area marks resonances assigned to surface phosphates.

## Identification of intermediate sodiated phases

The presence of more crystallized phases, as described by Mayo et al. [2] from calculations, was nevertheless tracked down in the phosphorus spectra. Phases such as $Na_3P_7$ and $Na_3P_{11}$ are indeed characterized by $^{23}Na$ MAS NMR signals in the same chemical shift range. Considering first $^{31}P$ MAS NMR spectra of the 63 wt% electrode since the spectra are less crowded, while $Na_3P_{11}$ ($Na_{0.273}P$) calculated resonances at -245 and -266 ppm could be masked by the broad resonance at -245 ppm in the spectrum at the end of the second discharge, more intense calculated $Na_3P_{11}$ resonances at 150 and 170 ppm are obviously not observed in our experimental spectra. Note that calculated resonances at -240 and -270 ppm, corresponding to the most sodiated phosphorus environment might be also found in the amorphous $Na_{1-\alpha}P$, $Na_{2-\beta}P$ or $Na_{3-\gamma}P$. These last two resonances were observed experimentally by Morita et al. at -200 and -221 ppm. Again, no clear evidence of these two resonances could be found in our experimental spectra even though a -200 ppm signal could be masked by the -280 ppm signal of $Na_3P$ (for the electrode at

the end of the first discharge) and a -221 ppm signal could by masked by the broad signals in this region (for electrodes stopped at the end of the first or second discharge).

Similarly, $Na_3P_7$ ($Na_{0.429}P$) resonances calculated between -57 and -188 ppm [2] or observed between -44 and -160 ppm [1] cannot be observed on our experimental spectra.

Spectra obtained for the 74wt% electrodes at the end of the first and second discharge are more complex due to the high number of resonances and sidebands. Most of the calculated [2] and previously observed [1] $Na_3P_{11}$ resonances could be present and masked by the resonances we assigned to the amorphous $Na_{1-\alpha}P$, $Na_{2-\beta}P$ or $Na_{3-\gamma}P$. Nevertheless, the most intense calculated resonance for $Na_3P_{11}$ at 150 ppm would be expected to stand out, even if overlapping with the broad sideband we observe in this region. Similarly, most of the calculated or previously observed resonances for $Na_3P_7$, between -44 and -188 ppm, could be masked or overlapping with sidebands of resonances of $MnP_4$ or Na-P amorphous phases. Nevertheless, a set of 3 close-by resonances between -160 and -188 ppm would be expected, maybe appearing as one broad signals due to overlapping. Nevertheless, in this region, only a relatively sharp sideband of the resonance at -316 ppm. Overall, some Na and P environments similar to those in crystallized $Na_3P_7$ or $Na_3P_{11}$ could be present in the discharge electrodes but no clear evidence of the corresponding crystallized phases could be determined and our experimental results are more consistent with the presence of amorphous and disordered environments.

**Mn K-edge XAS: XANES analysis**

To better understand the evolution of the absorption edges during cycling and comparing them to those of Mn metal, one may look at the derivative of the absorption edges, which is shown in Figure SI 10a for pristine $MnP_4$, $MnP_4$ at EOD and bulk Mn metal.

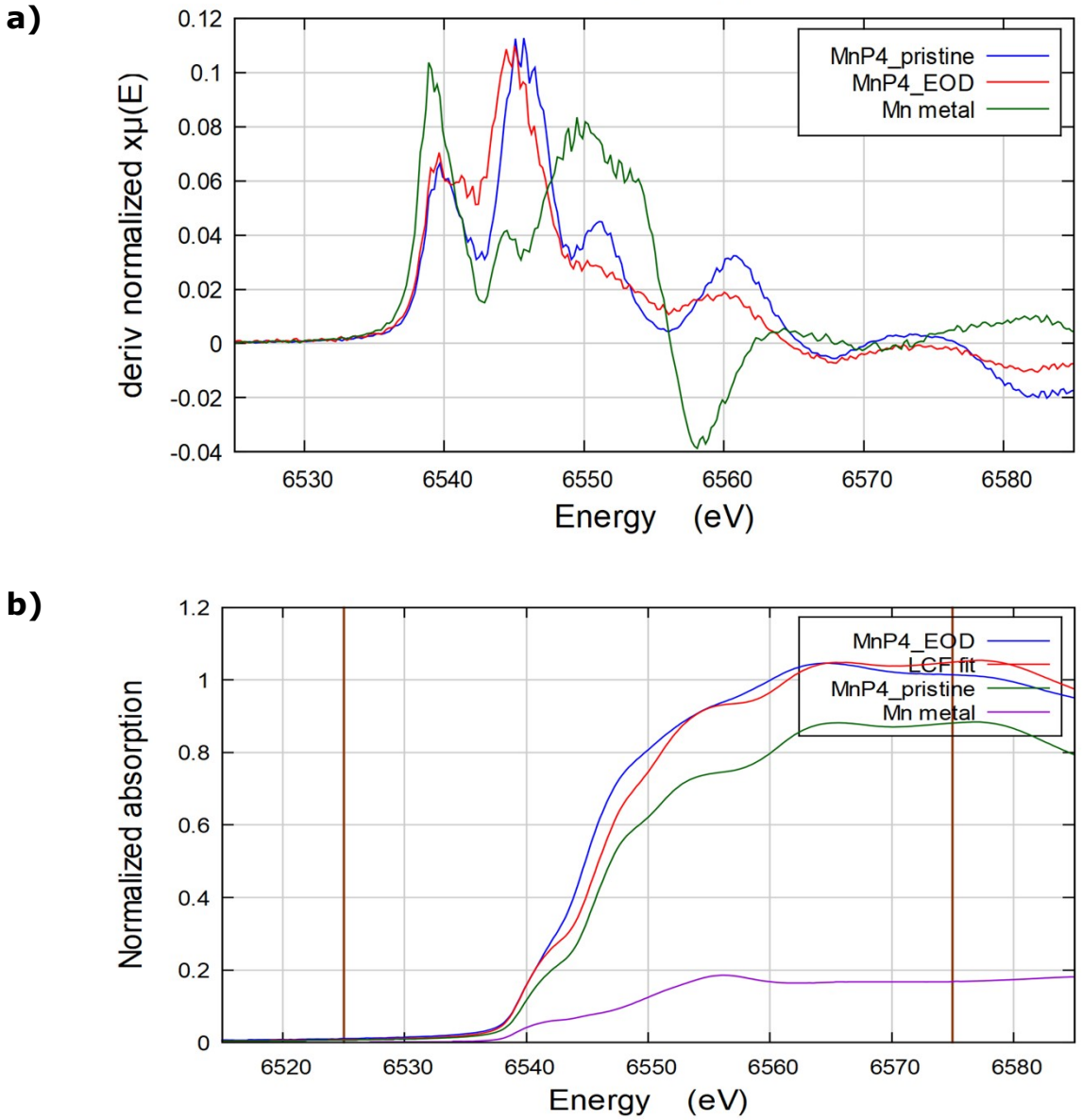


**Figure SI 10**: (a) First derivative of the absorption edges of pristine $MnP_4$, $MnP_4$ at EOD and Mn metal; (b) Linear combination fit of the absorption edge of MnP4 at EOD using pristine $MnP_4$ and Mn metal as references.

The first peak of the derivative for the different materials corresponds to the first inflection of the absorption edge, where usually the absorption edge position is set for the bulk metal. For all shown materials, this peak sits around 6539 eV, the typical value of Mn metal. In the case of $MnP_4$ at EOD, this peak is even more intense (though more

spread out) than for pristine $MnP_4$, in good agreement with the formation of some Mn metal during the conversion reaction.

An additional proof for the formation of Mn metal during the conversion reaction can be obtained by the linear combination fit of the spectrum of $MnP_4$ at EOD using a linear combination of the absorption edges of pristine $MnP_4$ and bulk Mn metal. The results of this fit (Figure SI 10b) indicate that more than 20% of Mn metal is contained in the sample. In the case of the sample at EOD after two cycles, this conversion increases up to almost 30% (not shown).

It must be underlined that such fittings are not precise, mainly because the reference used for the metal component is not perfectly adequate. In fact, as mentioned above, typical conversion reactions usually lead to the formation of very small metal particles (with sizes below 2 nm), which have a very large fraction of non-homogeneous chemical environments (surface, subsurface and core atoms, possible interactions with the external environment, etc.) inducing the loss of spectral features in the absorption edge. For this reason, these results should be considered as tentative fits. In spite of their imprecision, however, these results agree well with the EXAFS fits reported in the manuscript and shown in Figure SI 11.

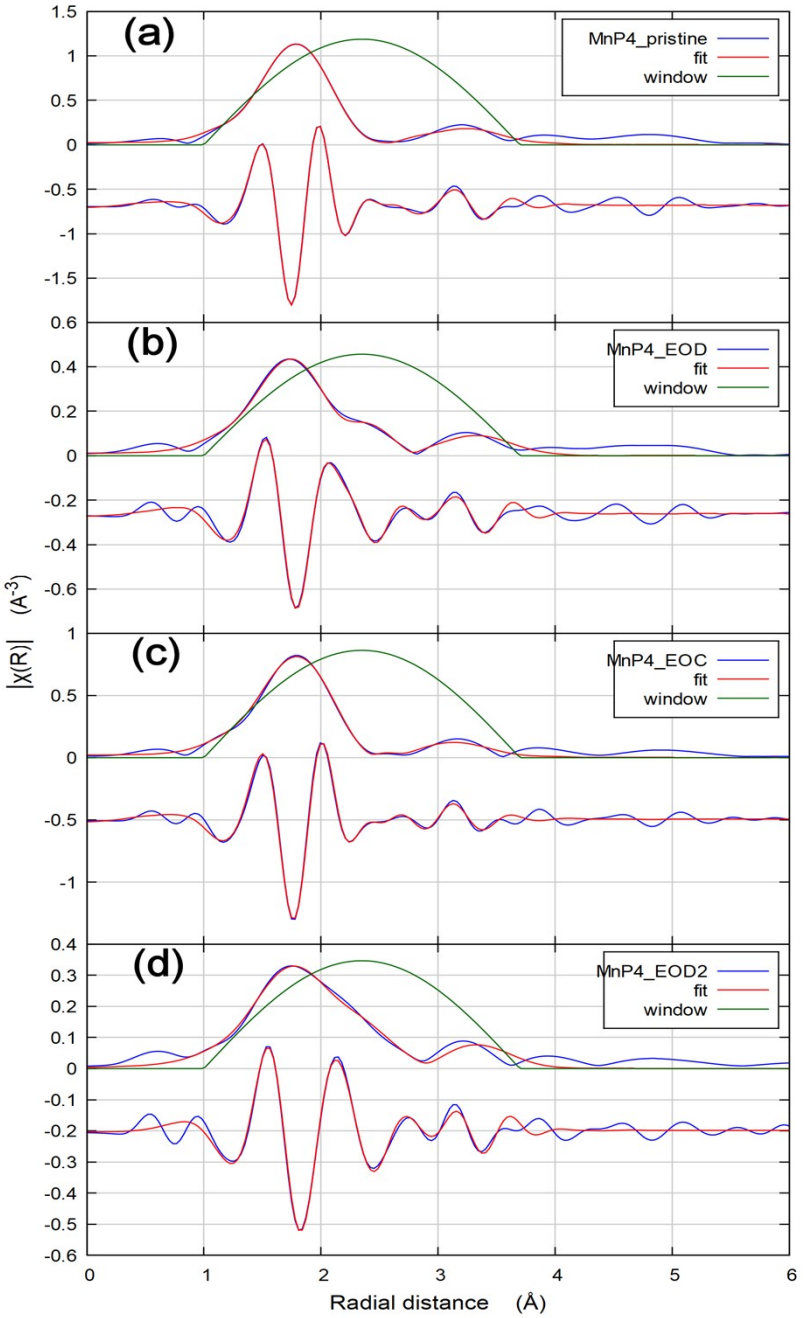


**Figure SI 11**: Fitted EXAS spectra of the $MnP_4$ electrodes at different states of charge and discharge: (a) pristine, (b) end of first discharge, (c) end of first charge and (d) and of second discharge

[1]: Ryohei Morita, Kazuma Gotoh, Mouad Dahbi, Kei Kubota, Shinichi Komaba, Kazuyasu Tokiwa, Saeid Arabnejad, Koichi Yamashita, Kenzo Deguchi, Shinobu Ohki, Tadashi Shimizu, Robert Laskowski, Hiroyuki Ishida, Journal of Power Sources 413 (2019) 418–424
[2]: Martin Mayo, Kent J. Griffith, Chris J. Pickard, Andrew J. Morris, Chem. Mater. 2016, 28, 2011−2021